

Supplementary information for

**Accelerated  $^{19}\text{F}$  biomolecular magic-angle spinning NMR with  
paramagnetic dopants**

Lea M. Becker<sup>[a]</sup>, Giorgia Toscano<sup>[a,b]</sup>, Anna Kapitonova<sup>[a]</sup>, Rajkumar Singh<sup>[a]</sup>, Undina Guillerm<sup>[a]</sup>, Roman Lichtenecker<sup>[b]</sup>,  
and Paul Schanda\*<sup>[a]</sup>

---

[a] L. M. Becker, A. Kapitonova, P. Schanda\*

Institute of Science and Technology Austria, Am Campus 1, 3400 Klosterneuburg, Austria

E-mail: paul.schanda@ista.ac.at

[b] G. Toscano, R. Lichtenecker

Institute of Organic Chemistry, University of Vienna, Währinger Str. 38, 1090 Vienna, Austria

---

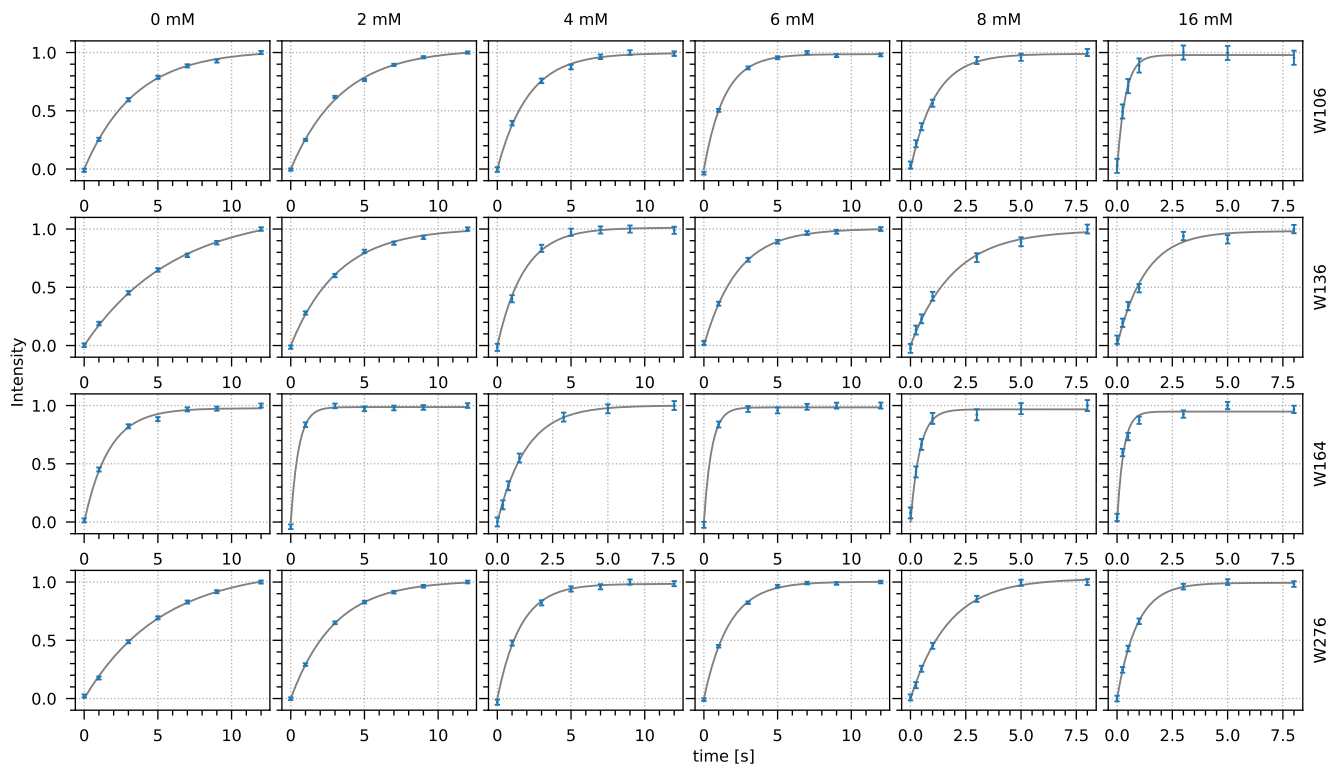


**Figure S1:** Residue-wise exponential fits of  $^{19}\text{F}$   $R_1$  saturation-recovery relaxation experiments (Fig. 1b) at seven different concentrations of Gd(DTPA-BMA). Concentrations and residues are indicated on the top and at the right side, respectively.

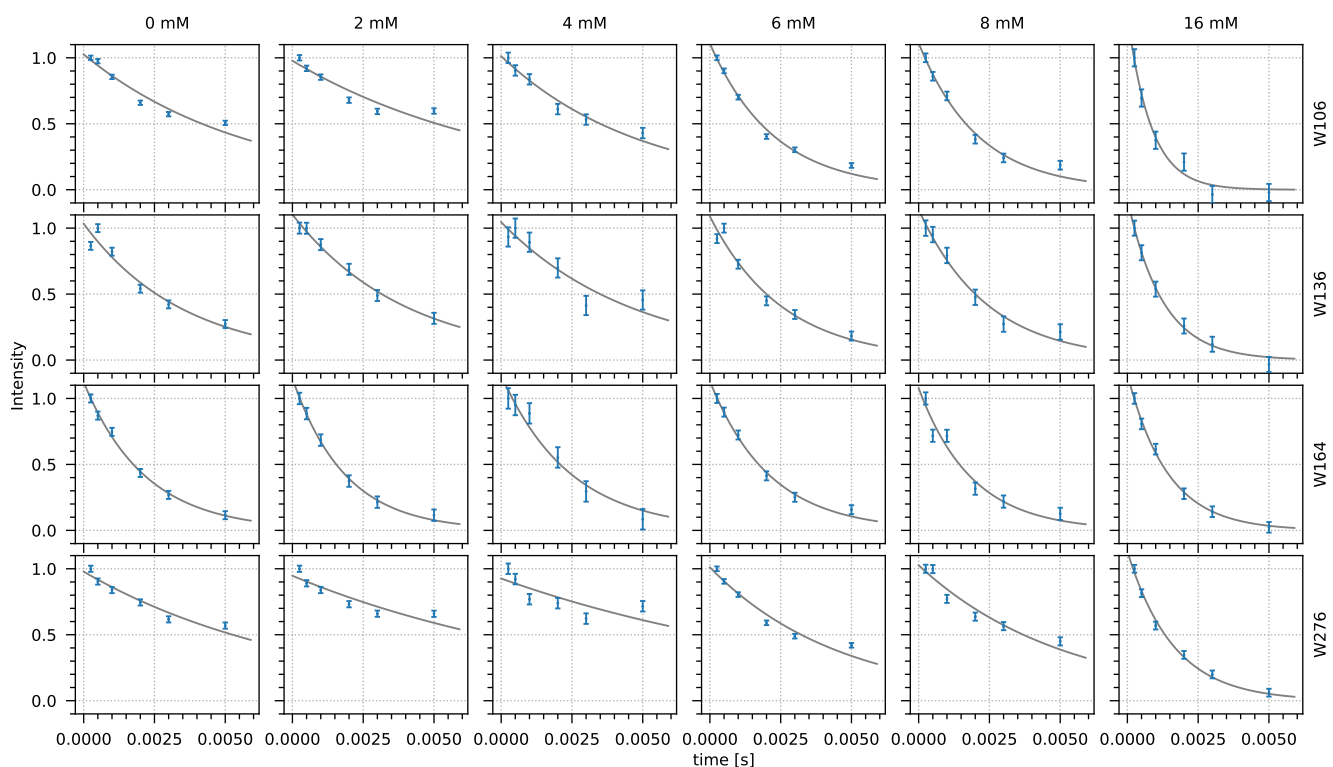


**Figure S2:** Residue-wise exponential fits of  $^{19}\text{F}$   $R_2$  relaxation experiments (Fig. 1c) at seven different concentrations of Gd(DTPA-BMA). Concentrations and residues are indicated on the top and at the right side, respectively.

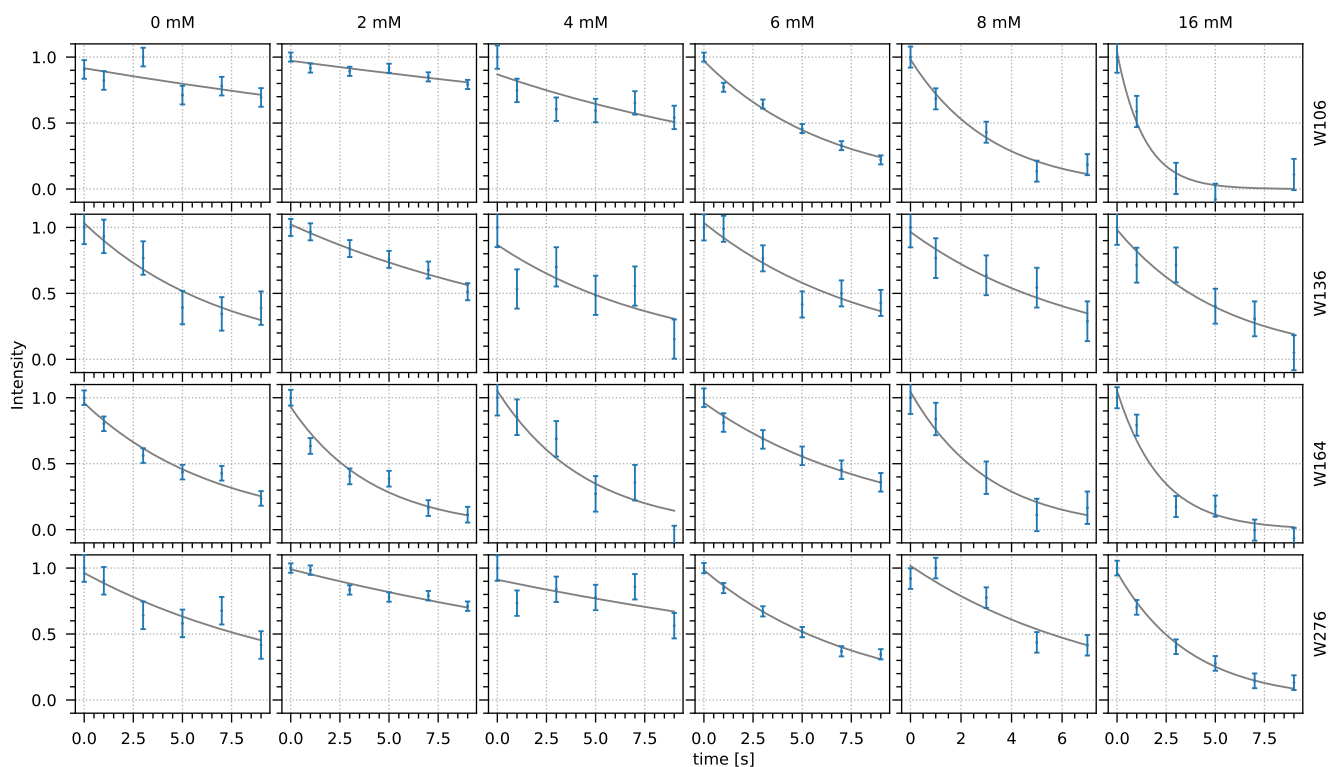


**Figure S3:** Residue-wise exponential fits of  $^{13}\text{C}$   $R_1$  relaxation experiments (Fig. 1d) at seven different concentrations of Gd(DTPA-BMA). Concentrations and residues are indicated on the top and at the right side, respectively.

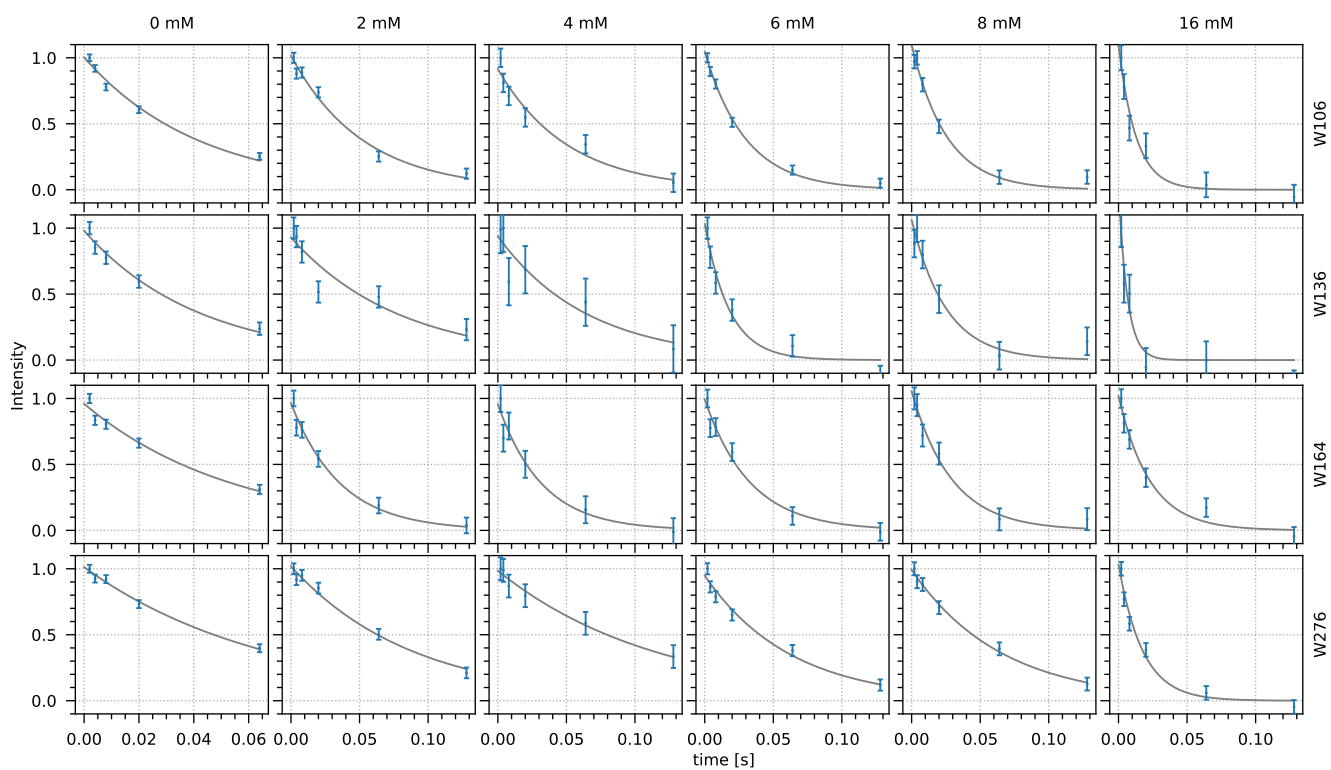


**Figure S4:** Residue-wise exponential fits of  $^{13}\text{C}$   $R_2$  relaxation experiments (Fig. 1e) at seven different concentrations of Gd(DTPA-BMA). Concentrations and residues are indicated on the top and at the right side, respectively.

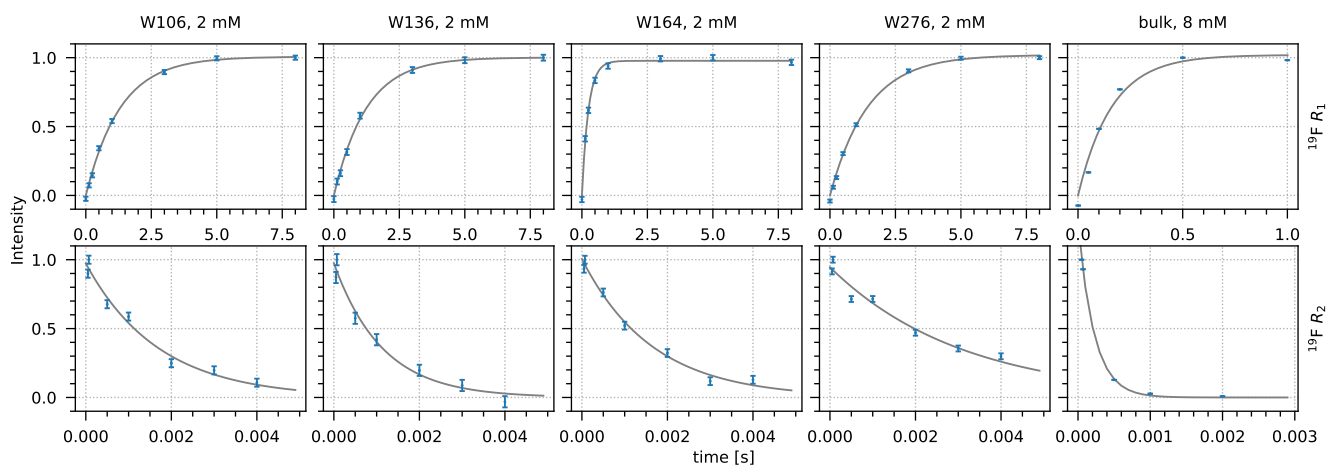


**Figure S5:** Exponential fits of  $^{19}\text{F}$   $R_1$  (top) and  $R_2$  (bottom) relaxation experiments (Fig. 1b,c) at two different concentrations of Gd(DTPA). The first four columns are residue-wise fits at 2 mM Gd(DTPA). The last column is a fit of the bulk signal at 8 mM Gd(DTPA), as the signals were not resolved due to broadening.

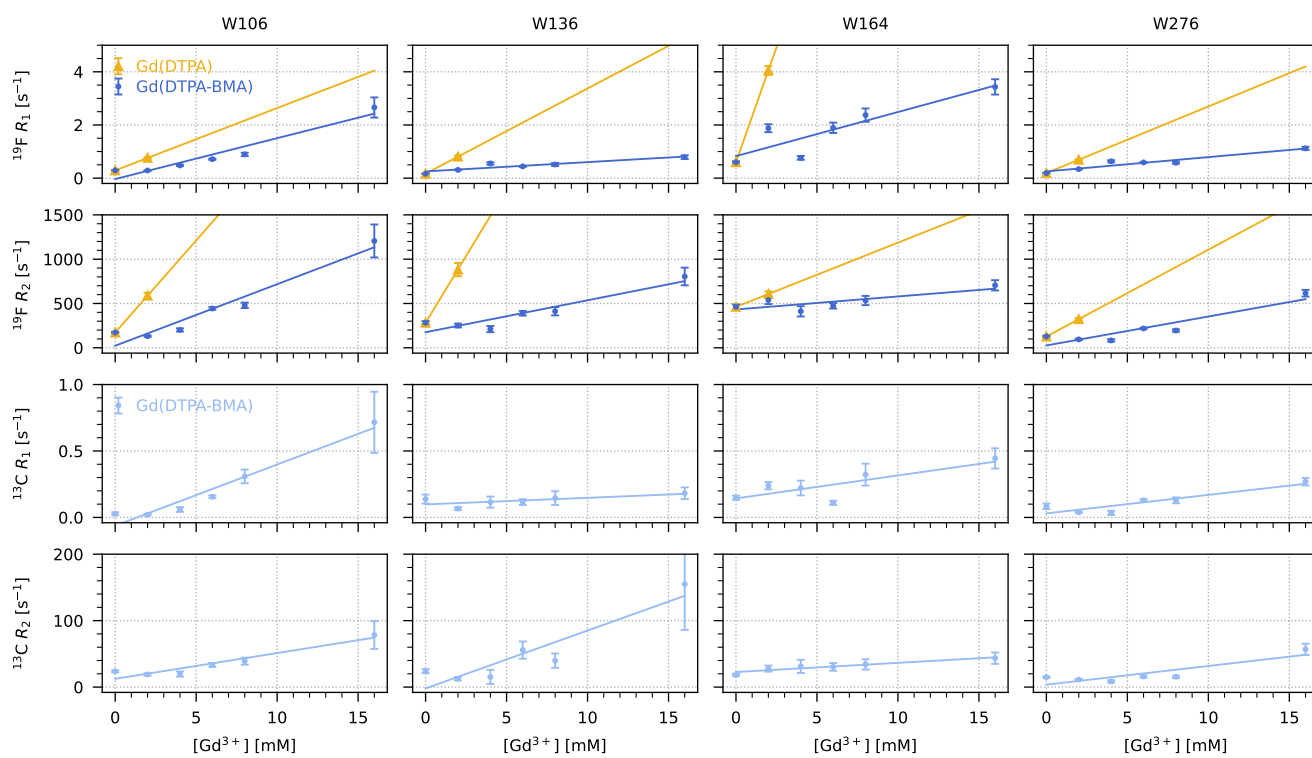


**Figure S6:** Linear fits of  $^{19}\text{F}$  and  $^{13}\text{C}$   $R_1$  and  $R_2$  relaxation rates (see y-axis labels) as a function of the concentration of Gd(DTPA-BMA) and Gd(DTPA) for each tryptophan (indicated on the top).

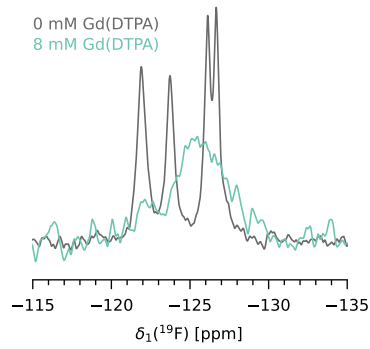


**Figure S7:** 1D  $^{19}\text{F}$  MAS NMR spectrum of 5FC-W-TET without (gray) and with 8 mM Gd(DTPA) (cyan).

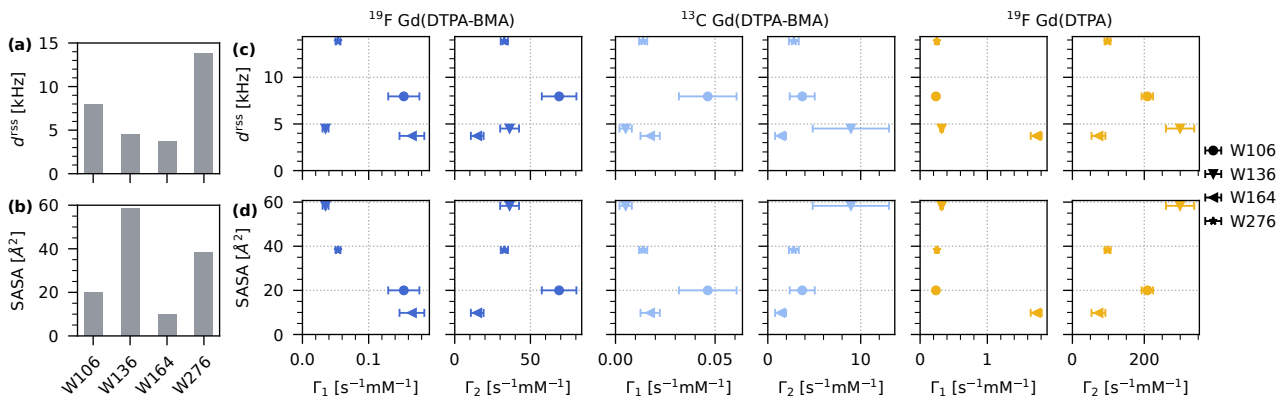


**Figure S8:** Analysis of tryptophan environments in TET2. (a) Strength of the dipolar coupling network  $d^{TSS}$  for each tryptophan. All exchangeable protons and all protons of phenylalanines and tyrosines were considered, and distances for the calculations were based on PDB ID 1Y0R ((1)). (b) Surface accessible surface area (SASA) of tryptophans. The SASA was determined with the `gmx sasa` function implemented in GROMACS 2023.5 ((2)) with a probe radius of 1.4 nm. (c) Correlations between  $d^{TSS}$  and  $\Gamma_1$  and  $\Gamma_2$ . (d) Correlations between SASA and  $\Gamma_1$  and  $\Gamma_2$ .

## References

- (1) Borissenko, L., and Groll, M. (2005). Crystal structure of TET protease reveals complementary protein degradation pathways in prokaryotes. *J. Mol. Biol.* 346, 1207–1219.
- (2) Abraham, M. J. et al. (2015). GROMACS: High performance molecular simulations through multi-level parallelism from laptops to supercomputers. *SoftwareX* 1-2, 19–25.